Sr$_3$Ti$_2$O$_7$ Ruddlesden−Popper Phase Synthesis by Milling Routes

T. Hungría, J. G. Lisoni,[†] and A. Castro*

Instituto de Ciencia de Materiales de Madrid, CSIC, Cantoblanco, 28049 Madrid, Spain

This paper presents a new method of synthesis, mechanochemical activation, for the preparation of the Sr$_3$Ti$_2$O$_7$ Ruddlesden−Popper (RP) phase. The results obtained from different starting reagents (SrO, SrCO$_3$, or Sr(OH)$_2$·8H$_2$O and TiO$_2$ anatase) and mechanical activation systems (vibrating and planetary mills) are compared. An optimized protocol is established that permits one to avoid the high temperatures and long reaction times needed in the classical solid-state reaction method; as a byproduct, very pure phases with controlled particle sizes are isolated as well. The products were studied by X-ray diffraction at room temperature and above, thermal analysis techniques, infrared spectroscopy, and scanning electron microscopy. The insight obtained in this work can be extrapolated to other Sr$_2$[Sr$_{n-1}$Ti$_n$O$_{3n+1}$] Ruddlesden−Popper materials that have not been isolated, until now, as single phases.

Introduction

The Ruddlesden−Popper (RP) structural type is built up from perovskite-like blocks, *n* octahedra thick, interleaved by A cations along one of the cubic directions of the perovskite structure, yielding phases with the general formula A$_2$[A$_{n-1}$B$_n$O$_{3n+1}$], where $1 \leq n \leq \infty$[1,2] (the conventional ABO$_3$ perovskite has $n = \infty$). There is much interest in the physical properties and structural chemistry of perovskite-layered compounds because of their wide range of applications such as magnetic materials[3], high-temperature superconductors,[4] catalysts,[5] and electrode materials,[6] among others. The Ruddlesden−Popper Sr$_2$[Sr$_{n-1}$Ti$_n$O$_{3n+1}$] series constitute the prototype of these materials, where Sr$_2$TiO$_4$, Sr$_3$Ti$_2$O$_7$, Sr$_4$Ti$_3$O$_{10}$, and SrTiO$_3$ represent the members for $n = 1$, 2, 3, and ∞, respectively. SrTiO$_3$ exhibits a wide range of electrical behaviors: from a high-dielectric-constant material to a metallic superconductor when doped with a variety of elements. It has been studied as a substrate for perovskite oxides and for applications in tunable dielectric devices.[7,8] This broad range of physical properties and applications of SrTiO$_3$ make the investigation of other members of this homologous series

an obvious step in the search for new materials with improved properties.[9]

Conventional ceramic synthesis has been the most widely applied method for the preparation of these oxides, but it requires high temperatures and long reaction times. Moreover, it yields products with large and inhomogeneous particle sizes, and it is difficult to produce the desired materials in a controllable way. Therefore, alternative routes need to be developed to facilitate the reactions in the solid state.

The first five members of the Sr$_2$[Sr$_{n-1}$Ti$_n$O$_{3n+1}$] homologous series have been grown as thin films by reactive molecular epitaxy on SrTiO$_3$(001) substrates. The films were epitaxially oriented and were free of intergrowths for $n = 1-3$ but not for $n = 4$, 5.[9,10]

Mechanoactivation techniques have been mainly used for the synthesis of intermetallics and alloy compounds.[11] Recently, they have also been employed for the preparation of amorphous and nanocrystalline materials,[12,13] as well as in the synthesis of new compounds and in the improvement of their physicochemical characteristics.[14−20]

* Corresponding author: Dr. A. Castro, Instituto de Ciencia de Materiales de Madrid, CSIC, Cantoblanco, 28049 Madrid, Spain. Tel.: (+34) 91 334 9000. Fax: (+34) 91 372 0623. E-mail: acastro@ icmm.csic.es.

† Present address: IMEC, Kapeldreef 75, 3001 Leuven, Belgium.

(1) Ruddlesden, S. N.; Popper, P. *Acta Crystallogr.* **1957,** *10,* 538.
(2) Ruddlesden, S. N.; Popper, P. *Acta Crystallogr.* **1958,** *11,* 54.
(3) Mahesh, R.; Mahendiran, R.; Raychaudhuri, A. K.; Rao, C. N. R. *J. Solid State Chem.* **1996,** *122,* 448.
(4) Cava, J.; Van Dover, R. B.; Batlogg, B.; Rietmann, E. A. *Phys. Rev. Lett.* **1987,** *58,* 408.
(5) Voorhove, R. J. H.; Johnson, D. W.; Remeika, P.; Gallagher, P. K. *Science* **1977,** *195,* 827.
(6) Meadowcraft, D. B. *Nature* **1970,** *226,* 847.
(7) Van Keuls, F. W.; Romanofsky, R. R.; Bohman, D. Y.; Winters, M. D.; Miranda F. A. *Appl. Phy. Lett.* **1997,** *71,* 3075.
(8) Xi, X. X.; Li, H.-C. Si, W.; Sirenko, A. A.; Akimov, I. A.; Fox, J. R.; Clark, A. M.; Hao, J. *J. Electroceram.* **2000,** *4,* 393.

(9) Haeni, J. H.; Theis, C. D.; Schlom, D. G.; Tian, W.; Pan, X. Q.; Chang, H.; Takeuchi, I.; Xiang, X.-D. *Appl. Phys. Lett.* **2001,** *78,* 3292.
(10) Tian, W.; Pan, X. Q.; Haeni, J. H.; Scholm, D. G. *J. Mater. Res.* **2001,** *16,* 2013.
(11) Benjamin, J. S. *Sci. Am.* **1976,** *234,* 40.
(12) Ding, J.; Miao, W. F.; McCormick, P. G.; Street, R. *Appl. Phys. Lett.* **1995,** *67,* 3804.
(13) Giri, A. K. *Adv. Mater.* **1997,** *9,* 163.
(14) Lisoni, J. G.; Millán, P.; Vila, E.; Martín de Vidales, J. L.; Hoffmann, T.; Castro, A. *Chem. Mater.* **2001,** *13,* 2084.
(15) Lacorre, P.; Retoux, R. *J. Solid State Chem.* **1997,** *132,* 443.
(16) Castro, A.; Millán, P.; Ricote, J.; Pardo, L. *J. Mater. Chem.* **2000,** *10,* 767.
(17) González-Calbet, J. M.; Alonso, J.; Herrero, E.; Vallet-Regí, M. *Solid State Ionics,* **1997,** *101−103,* 119.
(18) Jiang, M. G.; Perez, R. J.; Lau, M. L.; Lavernia, E. J. *J. Mater. Res.* **1997,** *12,* 1429.
(19) Castro, A.; Millán, P.; Pardo, L.; Jiménez., B. *J. Mater. Chem.* **1999,** *9,* 1313.
(20) Kodakov, G. S. *Colloid J.* **1994,** *56,* 84.

During mechanical treatment, materials are comminuted; the homogeneity of the mixture is increased; the size of the crystallites is reduced; the crystal structure is damaged; and, in most of cases, the mechanically activated materials become more reactive and capable of faster reaction.[21,22] Consequently, the necessary calcination step to form the designed phase is completed at a lower temperature and in a shorter time than in the traditional ceramic method. Moreover, in some cases, the formation of the desired phase is observed during the mechanical treatment; that is, it is mechanosynthesized. In particular, titanates of the general formula $MTiO_3$ (M = Ca, Sr, and Ba) have been obtained directly by mechanosynthesis from alkaline-earth oxides and rutile in a vertical stainless steel ball mill at room temperature.[23]

More recently, Berbenni et al.[24] attempted to synthesize $Sr_2[Sr_{n-1}Ti_nO_{3n+1}]$ compounds with $n = 1-3$ by mechanical activation of stoichiometric mixtures of $SrCO_3$ and TiO_2 (rutile). $SrTiO_3$ and Sr_2TiO_4 were obtained after annealing for 12 h at 800–850 °C from mechanically activated precursors. On the contrary, no $Sr_3Ti_2O_7$ was shown to form by the same procedure.

In this paper, we study for the first time the synthesis of the $Sr_3Ti_2O_7$ RP phase ($n = 2$), obtained after calcination of stoichiometric mixtures of the mechano-activated Sr components and TiO_2. A comparative investigation is carried out using different strontium initial reagents [SrO, $Sr(OH)_2 \cdot 8H_2O$, and $SrCO_3$] and milling systems (vibrating and planetary mills). It is shown that the synthesis protocols are vastly improved, producing a decrease in the reaction temperature and time, as compared with the traditional solid-state method requirements of about 450 °C and at least 1 week. Moreover, the mesostructure of the produced samples is studied.

Experimental Procedure

Mechanical activation techniques have been applied to the synthesis of the $Sr_3Ti_2O_7$ RP phase. In all cases, the same procedure was followed: A stoichiometric mixture of analytical-grade TiO_2 (anatase) and strontium starting materials (SrO, $SrCO_3$, and $Sr(OH)_2 \cdot 8H_2O$) was initially homogenized by hand in an agate mortar. Then, the mixtures were activated by different milling techniques and, finally, calcined in one step to obtain $Sr_3Ti_2O_7$. Special care was taken with the strontium oxide precursor, because of its high instability in air. It was stored in a glovebox under controlled argon atmosphere, and the necessary quantities for the initial mixtures were weighed inside this box. Afterward, the measured quantities were immediately mixed with TiO_2 and quickly put in the mill. No special atmospheres were used during grinding.

For the sake of comparison, $Sr_3Ti_2O_7$ RP powders were also synthesized by the traditional ceramic route. In that case, a stoichiometric $SrCO_3$ or $Sr(OH)_2 \cdot 8H_2O$ and TiO_2 mixture was treated at increasing temperature from 500 to 1250 °C, with each temperature maintained for different times; cooled by quenching; weighed; reground; and examined by X-ray diffraction.

(21) Isobe, T.; Serna, M. *J. Solid State Chem.* **1991**, *93*, 358.
(22) Vidojkovic, V. M.; Braukovic, A. R.; Milosevic, S. D. *Mater. Lett.* **1997**, *31*, 55.
(23) Welham, N. J. *J. Mater. Res.* **1998**, *13*, 1607.
(24) Berbenni, V.; Marini, A.; Bruni, G. *J. Alloys Compd.* **2001**, *329*, 230.

Vibrating and planetary mills (Fritsch, Pulverisette models 0 and 6, respectively) were used for the mechanical activation. In both cases, the initial mixture was placed in a stainless steel vessel with balls of the same material. In the vibrating mill, one ball of 5-cm diameter was used, whereas, in the planetary mill, five balls of 1-cm diameter each were utilized. The grinding bowl of the planetary mill was rotated at 200 rpm. The ball/powder weight ratio was about 16:1.

X-ray diffraction (XRD) patterns at room temperature were recorded with a Siemens D-501 diffractometer. The patterns were collected in the range of 5–60° (2θ), with scan rates of 0.05°/s. At higher temperatures, a Philips PW1310 diffractometer fitted with an Anton Paar HTK 10 attachment was used to stabilize the temperature during the measurements. The diffractograms were obtained by depositing a small quantity of powder onto a platinum sheet placed on a tantalum strip, which was the heating element. The recordings were taken from 5 to 70° (2θ) with a scan rate of 0.02°/s. The temperature was monitored by a Pt–Pt 13% Rh thermocouple welded in the center of the platinum sheet. The heating rate was 10 °C min^{-1}, and the temperature was stabilized for 1 h. The Cu Kα doublet ($\lambda = 0.15418$ nm) was used in all X-ray experiments.

The thermal behavior was investigated by differential thermal analysis (DTA) and thermogravimetric (TG) analysis. The measurements were carried out in air, from room temperature to 1200 °C using a Seiko 320 instrument with α-Al_2O_3 as the inert reference material. The heating and cooling rates were 10 °C min^{-1}, and the quantity of sample used was about 10 mg.

Infrared absorption spectra were recorded from 400 to 4000 cm^{-1} using a Nicolet 20SXC FT-IR spectrometer.

SEM images were taken at 3 kV in a Philips SFEG-XL30 microscope. For this purpose, suspensions of the powders in ethanol were precipitated onto a smooth silicon surface. No additional gold layer was sputtered on. To obtain an ultra-high-resolution image of the surface topography, a through-the-lens-detector mode was used.

Results and Discussion

Table 1 summarizes the phases identified after mechanical and thermal treatments of as-mixed and mechanochemically activated $3SrO/2TiO_2$, $3SrCO_3/2TiO_2$, and $3Sr(OH)_2 \cdot 8H_2O/2TiO_2$ samples.

SrO Reagent. Figure 1a shows the XRD patterns of the $3SrO/2TiO_2$ mixture treated in the vibrating mill for increasing times. After the first 7 days of mechanical activation, the formation of $SrTiO_3$ started, although a small amount of SrO was still observed. $SrTiO_3$ was the unique detectable phase after 11 days of milling, and it remained stable after longer grinding times. Its crystallite size estimated from the full width at half-maximum (B) of the (110) $SrTiO_3$ peak was approximately 10 nm [using the Scherrer formula $\xi = 0.98\lambda_{CuK\alpha}/(B \cos \theta_0)$[25]]. Despite the high reactivity of SrO with H_2O and CO_2 in the air, no $SrCO_3$ was detected.

TG tracing, acquired from a heating/cooling cycle of the powder milled for 11 days, displayed three weight-loss steps (Figure 2a): 2 wt % between room temperature and 300 °C, 0.6 wt % from 300 to 680 °C, and 3 wt % between 680 and 910 °C. The DTA curve exhibits only one endothermic peak on heating to 835 °C, corresponding to the important last weight-loss step. The TG and DTA recordings were interpreted on the basis of XRD data taken at increasing temperatures (Figure 3). There

(25) Cullity, B. D. *Elements of X-ray Diffraction*; Addison-Wesley Series in Metallurgy and Materials; Addison-Wesley: Reading, MA, 1967.

Table 1. Identified Phases after Mechanical Treatments in a Vibrating Mill and Thermal Annealings of Different Sr Reagents and Rutile Mixtures[a]

annealing temp/°C (annealing time/h)	identified phases[b]	
SrO		
		milling time = 11 days
RT[c]		$SrTiO_3 + SrCO_3$ (lc)
250 (12)		$SrTiO_3 + SrCO_3$ (lc)
600 (12)		$SrTiO_3 + SrCO_3$
800 (24)		$Sr_3Ti_2O_7$
1150 (12)		$Sr_3Ti_2O_7$
SrCO₃	milling time = 0 days	milling time = 42 days
RT[c]	$SrCO_3 + TiO_2$	$SrCO_3 + TiO_2$ (lc)
250 (12)	—	$SrCO_3 + TiO_2$ (lc)
600 (12)	—	$SrCO_3 + SrTiO_3$
700 (86)	$SrCO_3 + SrTiO_3 + TiO_2$	—
800 (24)	$SrTiO_3 + SrCO_3$	—
900 (24)	$SrTiO_3 + Sr_2TiO_4 + Sr_3Ti_2O_7$ (tr)	$Sr_2TiO_4 + Sr_3Ti_2O_7$
1000 (24)	$SrTiO_3 + Sr_2TiO_4 + Sr_3Ti_2O_7$	$Sr_3Ti_2O_7 + Sr_2TiO_4$
1250 (24)	$Sr_3Ti_2O_7 + Sr_2TiO_4$	$Sr_3Ti_2O_7 + Sr_2TiO_4$ (tr)
1250 (96)	$Sr_3Ti_2O_7 + Sr_2TiO_4$ (tr)	$Sr_3Ti_2O_7$
1250 (216)	$Sr_3Ti_2O_7$	
Sr(OH)₂·8H₂O	milling time = 0 days	milling time = 14 days
RT[c]	$SrCO_3 + TiO_2$	$SrCO_3 + SrTiO_3$
300 (12)	—	$SrCO_3 + SrTiO_3$
500 (12)	$SrCO_3 + Sr_2TiO_4$	$SrCO_3 + SrTiO_3$
700 (12)	$SrCO_3 + Sr_2TiO_4$	—
800 (12)	$Sr_2TiO_4 + SrTiO_3 + SrCO_3$	—
900 (24)	$Sr_2TiO_4 + SrTiO_3$	—
1000 (24)	$Sr_2TiO_4 + SrTiO_3$	$Sr_3Ti_2O_7 + Sr_2TiO_4$
1200 (24)	$Sr_2TiO_4 + SrTiO_3 + Sr_3Ti_2O_7$	—
1250 (24)	$Sr_3Ti_2O_7 + Sr_2TiO_4$	—
1250 (120)	—	$Sr_3Ti_2O_7 + SrTiO_3$ (tr)
1250 (196)	$Sr_3Ti_2O_7 + Sr_2TiO_4$ (tr)	
1250 (360)	$Sr_3Ti_2O_7$	

[a] Sr/Ti = 3/2. [b] lc = low crystallinity, tr = traces. [c] Room temperature.

were no noticeable changes up to 250 °C; however, $SrCO_3$ diffraction lines clearly appeared at temperatures above 500 °C and remained unaltered up to 700 °C. Beyond 800 °C, the doublet at $2\theta \approx 31°$, characteristic of $Sr_2[Sr_{n-1}Ti_nO_{3n+1}]$ RP oxides, started to become visible, but its relative intensity showed that the formation of $Sr_3Ti_2O_7$ had not been completed. Moreover, traces of Sr_2TiO_4 and $SrTiO_3$ were still observed at the final room temperature.

To isolate each stable phase at room temperature, the precursor milled for 11 days was heated in a furnace at temperatures similar to those used in the high temperature XRD technique. The heating treatments were finished by quenching in air (Table 1). The results obtained were comparable to those mentioned above. At 250 °C, the patterns were similar to those for the as-milled sample, where only the $SrTiO_3$ peaks were detected. The maximum weight loss measured at this temperature was 2.4 wt %, even when annealings longer than 12 h were carried out, which coincides with the results of TG (2 wt %). The $SrCO_3$ signals become observable at temperatures higher than 500 °C, which is well correlated with the second weight loss measured by TG (300−680 °C). It is interesting to note that the mechanoactivated powders annealed at 600 °C for 3 h or longer displayed a weight loss of ~1.4 wt %, this value being 60% higher than the one measured at 250 °C. This indicates that part of the SrO present in the as-milled powder has been carbonated to form $SrCO_3$, at the same time that some atmospheric water was incorporated to the system, which was later progressively lost from
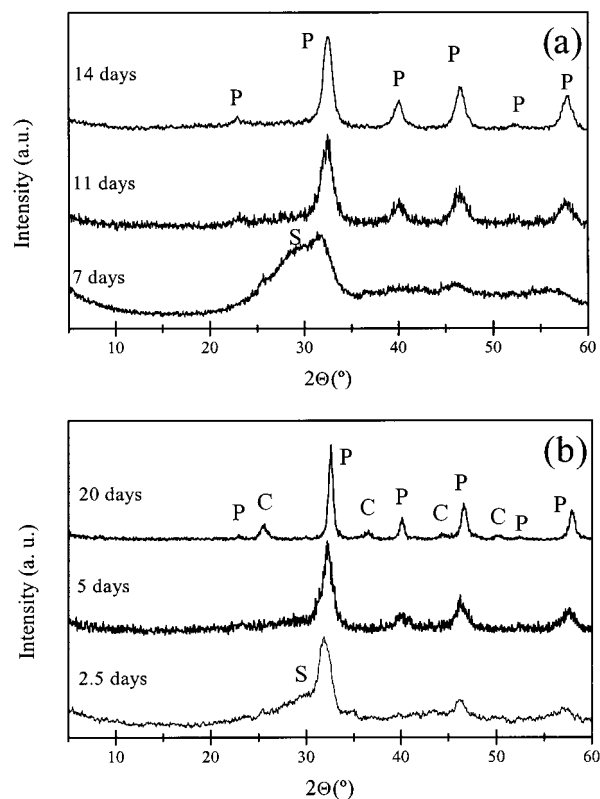

Figure 1. XRD patterns of the $3SrO/2TiO_2$ mixture after different activation times. The grinding was carried out by (a) vibrating and (b) planetary mills (S = SrO, P = $SrTiO_3$, and C = $SrCO_3$).
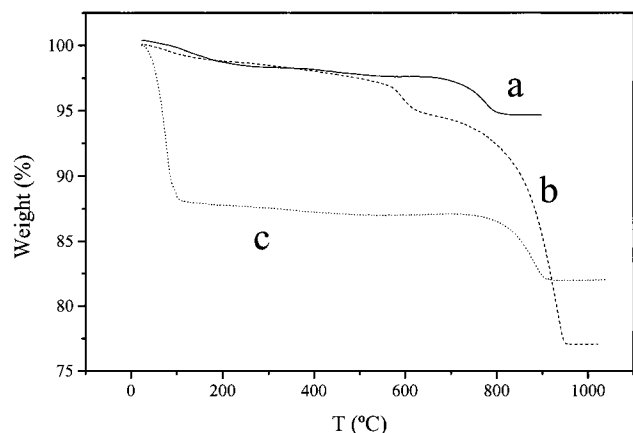
Figure 2. TG tracing of (a) a $3SrO/2TiO_2$ mixture mechano-activated for 11 days, (b) a $3SrCO_3/2TiO_2$ mixture milled for 42 days, and (c) a $3Sr(OH)_2 \cdot 8H_2O/2TiO_2$ mixture milled for 14 days, all of them in a vibrating system.
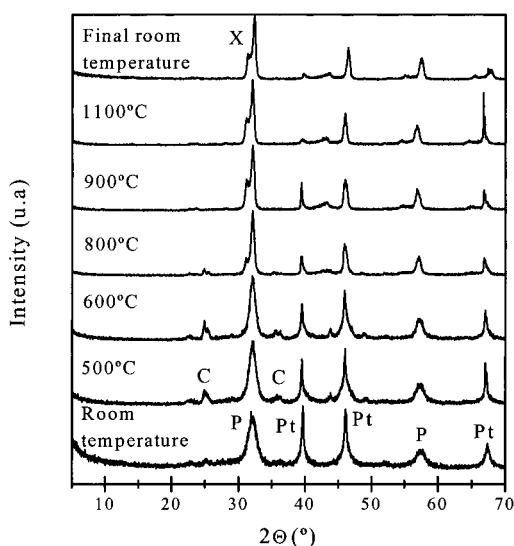

Figure 3. XRD patterns of a $3SrO/2TiO_2$ sample activated in a vibrating mill (11 days) at increasing temperatures (P = $SrTiO_3$, C = $SrCO_3$, Pt = platinum, and X = $Sr_3Ti_2O_7$ + Sr_2TiO_4 + $SrTiO_3$).

room temperature to 600 °C. $Sr_3Ti_2O_7$ was obtained as a single phase after a thermal treatment of 800 °C for 24 h. As the treatment temperature was increased to 1150 °C, shorter times were needed for $Sr_3Ti_2O_7$ formation, and an important crystallite growth from 20 to 30 nm was observed. Thus, the shortest time required for the $Sr_3Ti_2O_7$ formation was 12 h at 1150 °C, whereas the lowest temperature was 800 °C for 24 h.

IR investigations were carried out to detect the existence of H_2O and $CO_3{}^{2-}$ groups. Figure 4 shows the IR spectra of the powder mechanoactivated for 11 days and the samples annealed under different conditions. The as-milled powder displayed a single band at 600 cm^{-1}, corresponding to Ti—O bonds of $SrTiO_3$, as well as a very weak peak at 855 cm^{-1} and a doublet in the range of 1400—1450 cm^{-1} due to the δ(O—C—O) and ν(C—O) modes, respectively, of $SrCO_3$.[26] However, traces of H_2O could not be detected, perhaps because of its small quantity. A sample maintained at 600 °C for 12

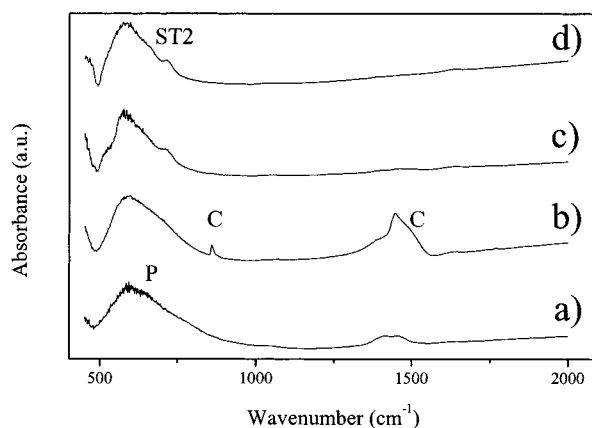(26) Nakamoto, K. *Infrared and Raman Spectra of Inorganic Compounds*; 4th ed.; John Wiley & Sons: New York, 1986; p 478.
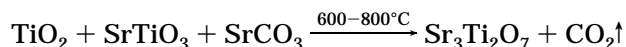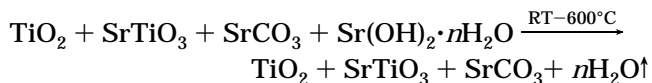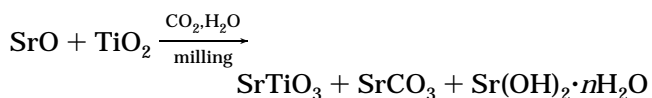

Figure 4. IR spectra after 11-day vibrating-mill treatment of the $3SrO/2TiO_2$ precursor (a) unannealed, (b) annealed at 600 °C for 12 h, and (c) annealed at 800 °C for 24 h and (d) of the $Sr_3Ti_2O_7$ phase obtained by solid-state reaction (P = $SrTiO_3$, C = $SrCO_3$, and ST2 = $Sr_3Ti_2O_7$).

h also showed the characteristic bands of $SrCO_3$ and $SrTiO_3$, those belonging to $SrCO_3$ being much more intense than those of the as-milled sample. This change in intensity is due to the crystallization of $SrCO_3$ during annealing. At 800 °C, $SrCO_3$ decomposes; $Sr_3Ti_2O_7$ appears; and, as one can observe in the IR spectra, only the typical doublet of $Sr_3Ti_2O_7$ Ruddlesden—Popper phase, at 700 and 570 cm^{-1}, is detected, corroborating the conclusion that this is the only phase present in the powder.

In summary, the results show that, in the formation of the $Sr_3Ti_2O_7$ RP phase, several processes are taking place during both mechanoactivation of the stoichiometric $3SrO/2TiO_2$ mixture and annealing treatments. During vibration milling, $SrTiO_3$ is mechanosynthesized, the powder takes in some water, and part of the SrO reacts with the CO_2 and H_2O of the air to form $SrCO_3$ and $Sr(OH)_2 \cdot nH_2O$. At this point, the only crystalline phase is $SrTiO_3$. The system seems to be saturated when a total increase of ~2.5 wt % has been reached. Water can be eliminated at temperatures below 600 °C. As the temperature increases, the $SrCO_3$ crystallites grow, and the compound clearly appears as a very crystalline phase at 600 °C. However, at temperatures higher than 800 °C, this phase decomposes by CO_2 elimination, this step being mainly defined by kinetic factors. Finally, SrO reacts with $SrTiO_3$ to form $Sr_3Ti_2O_7$. Another probable reaction mechanism is the intermediate formation of Sr_2TiO_4, which was only detected in the high-temperature XRD experiments. In conclusion, the chemical reactions occurring can be understood as follows

$$SrO + TiO_2 \xrightarrow[\text{milling}]{CO_2, H_2O}$$
$$SrTiO_3 + SrCO_3 + Sr(OH)_2 \cdot nH_2O$$

$$TiO_2 + SrTiO_3 + SrCO_3 + Sr(OH)_2 \cdot nH_2O \xrightarrow{RT-600°C}$$
$$TiO_2 + SrTiO_3 + SrCO_3 + nH_2O\uparrow$$

$$TiO_2 + SrTiO_3 + SrCO_3 \xrightarrow{600-800°C} Sr_3Ti_2O_7 + CO_2\uparrow$$

When a planetary mill is used, results similar to those mentioned above are obtained, although the time scales

involved to obtain the activated precursors are shorter. Figure 1b shows the XRD patterns of 3SrO/2TiO$_2$ mixture at increasing milling times in this system. After 2.5 days of milling, the mechanosynthesis of SrTiO$_3$ has already begun and a small amount of SrO is still observed. A few hours of further milling produces an abrupt increase in the SrTiO$_3$ peak intensities and the absence of crystalline SrO, which is no longer detected after 5 days of grinding. The most important differences with respect to the vibrating ball system were the growth of SrTiO$_3$ crystallites, whose size increased from 8 to 17 nm in powders ground for from 5 to 20 days, and the formation of crystalline SrCO$_3$ after 15 days of milling. Mechanosynthesis of Sr$_3$Ti$_2$O$_7$ was not observed upon longer milling times.

To make a comparative investigation of the thermal behavior of samples as a function of milling method, we investigated the sample milled for 5 days at the planetary mill. The choice of this product was based on the observation that it displayed the mechanosynthesis of SrTiO$_3$ and no detectable SrCO$_3$ formation, a behavior similar to that observed for the sample prepared in the vibrating mill system.

The only difference noticed in the two milling procedures was a weight increase of 0.8% at low temperatures on samples prepared in the planetary mill. This change cannot be correlated with any crystallographic transformation. This difference might be attributed to the higher temperatures reached in the planetary media (higher reactivity), which prevented atmospheric water from entering during the mechanical treatment. At higher temperatures, two weight losses of 0.3% between 240 and 600 °C and 2.6% from 700 to 900 °C were measured, which corresponded to SrCO$_3$ and Sr$_2$TiO$_4$ and Sr$_3$Ti$_2$O$_7$ RP phase formation, respectively. Similar conclusions were obtained from the X-ray powder patterns and IR spectra of the samples treated in the furnace at 250, 600, 800, and 1150 °C for different lengths of time. At 250 °C, no differences were observed between the as-milled and annealed powders, showing again that, at this temperature, only water elimination occurs. SrCO$_3$ was well crystallized at temperatures higher than 600 °C and remained stable up to 800 °C, at which point the Sr$_3$Ti$_2$O$_7$ RP oxide was formed as a single component after 24 h of annealing. The shortest time of treatment for obtaining Sr$_3$Ti$_2$O$_7$ was 12 h at 1150 °C.

SrCO$_3$ Reagent. When TiO$_2$ and SrCO$_3$ were used as the starting materials, even after 42 days of grinding, only the diffraction lines belonging to the reagents were detected, indicating that, if any reaction took place, it was under the XRD detection threshold. However, the significant broadening in the peaks showed that a diminution in crystallite sizes had been produced. Contrary to the results obtained when 3SrO/2TiO$_2$ powders were mechanoactivated, no mechanosynthesis of SrTiO$_3$ was detected.

Figure 2b depicts the thermal behavior of the mixture milled for 42 days. In the TG curve, three weight losses were observed: 2 wt % between room temperature and 200 °C, 5 wt % from 200 to 660 °C, and 15 wt % between 660 and 1000 °C. The DTA recordings exhibited two endothermic peaks on heating centered at 591 and 940 °C.
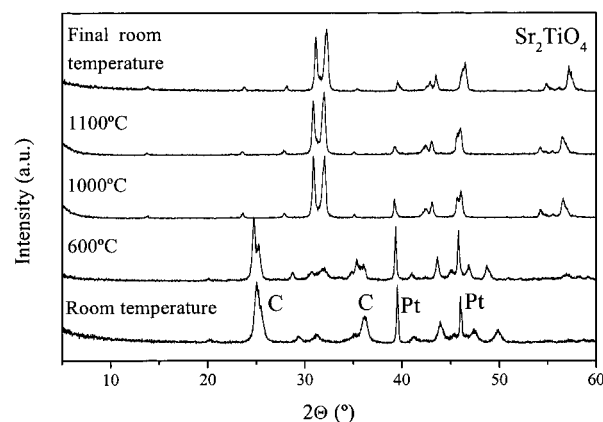

Figure 5. XRD recordings of 42-day-milled 3SrCO$_3$/2TiO$_2$ sample at increasing temperatures (C = SrCO$_3$ and Pt = platinum).

XRD at increasing temperatures (Figure 5) displayed no noticeable differences between the as-milled powders and those annealed at 200 °C. At 600 °C, a small peak at $2\theta \approx 31.9$ ° was detected, which corresponds to the onset of SrTiO$_3$ formation. At temperatures higher than 900 °C, SrCO$_3$ disappeared, and Sr$_2$TiO$_4$ signals became clearly visible. The final room temperature patterns showed that the sample was composed of only the Sr$_2$TiO$_4$ RP phase.

Similar results were obtained when the as-milled 3SrCO$_3$/2TiO$_2$ powders were furnace-annealed. No changes were detected in annealings carried out at 200 °C, which indicate that the first weight loss measured by TG corresponds to only water elimination. The most interesting transformation is observed at 600 °C, when the formation of SrTiO$_3$ was triggered, in good agreement with the first DTA peak detected at 591 °C. Moreover, isothermal TG curves obtained at this temperature for 1 h showed that the maximum weight loss was approximately 6 wt %, a value also corroborated by long furnace treatments. At temperatures higher than 900 °C, SrCO$_3$ completely decomposed, and the Sr$_2$TiO$_4$ and Sr$_3$Ti$_2$O$_7$ phases were clearly present, so that the second DTA peak observed at 940 °C can be attributed to crystallization of the RP phases. In this case, the Sr$_3$Ti$_2$O$_7$ RP phase was obtained as a single phase only in treatments performed at 1250 °C for at least 4 days, whereas lower temperatures or shorter times produced only a mixture of Sr$_2$TiO$_4$ and Sr$_3$Ti$_2$O$_7$.

In contrast to the reaction sequences proposed when the SrO reagent is used, the reactions involved with SrCO$_3$ are much simpler. In fact, the most important step is the elimination of the CO$_2$, followed by the reaction between SrO and TiO$_2$ to finally form the Sr$_3$Ti$_2$O$_7$ compound. Intermediate SrTiO$_3$ formation at 600 °C suggests that the process has already started even at this temperature, which is 100 °C lower than that observed in powders prepared by the traditional ceramic routes (Table 1).

No differences at all were noticed when a planetary mill was used, although a similar crystallite diminution was obtained after 1 day of grinding, instead of 42 days as in the case of the vibrating ball system. The mechanosynthesis of SrTiO$_3$ was not triggered, even when milling periods longer than 7 days were performed.

Sr(OH)$_2$·8H$_2$O Reagent. When Sr(OH)$_2$·8H$_2$O was used as the strontium source together with TiO$_2$, SrTiO$_3$
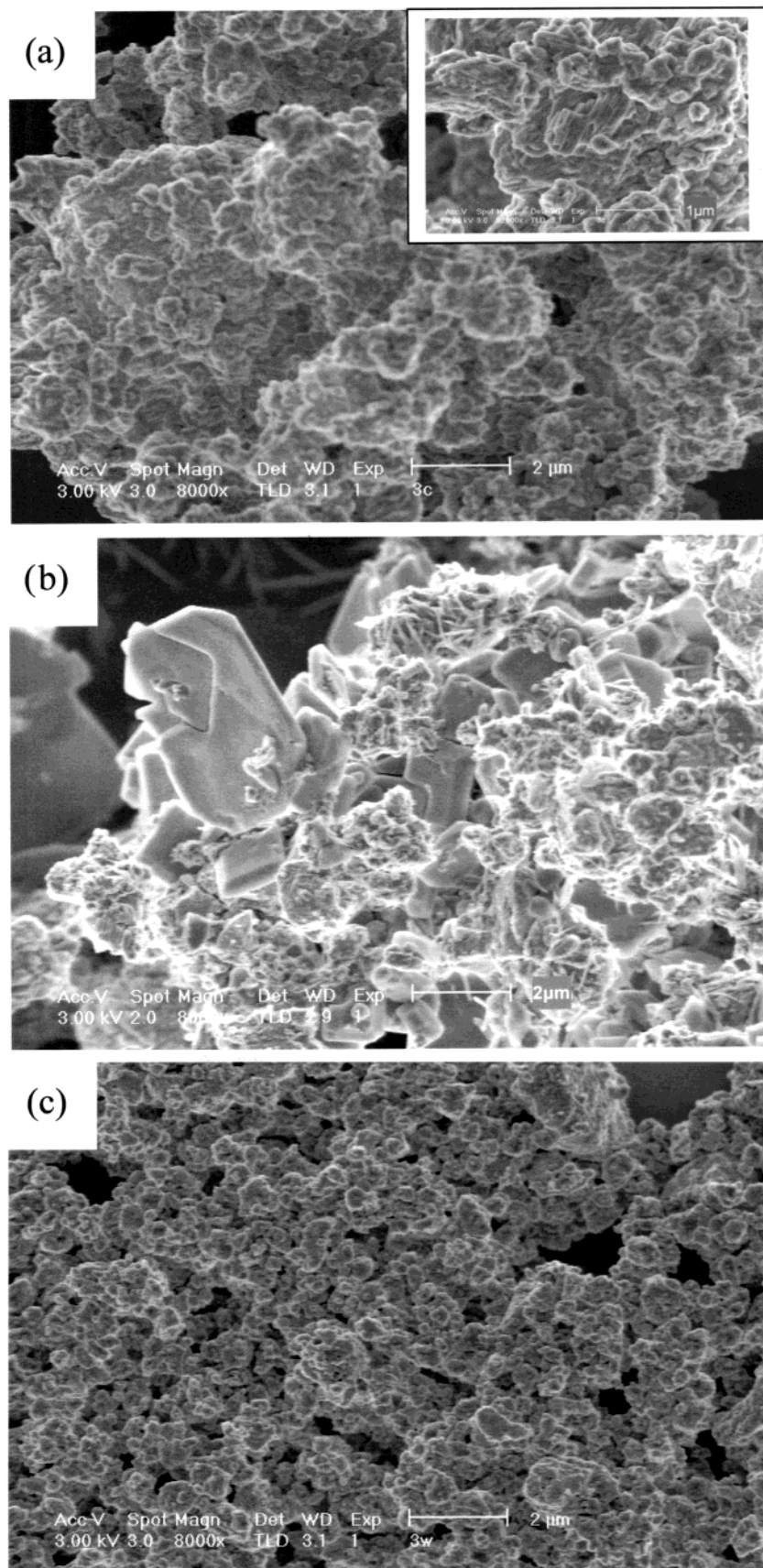
Figure 6. SEM micrographs of 3SrO/2TiO$_2$ mixture mechanoactivated for (a) 11 days and (b) 14 days using a vibrating system and (c) 7 days in a planetary mill.

peaks appeared after 9 days of vibrating-ball milling, although Sr(OH)$_2$·8H$_2$O diffraction lines were also present. When the Sr(OH)$_2$·8H$_2$O peaks could no longer

be detected, SrCO$_3$ became observable, as occurred in the final XRD patterns of the powders activated for 14 days. The SrTiO$_3$ crystallite size estimated from the
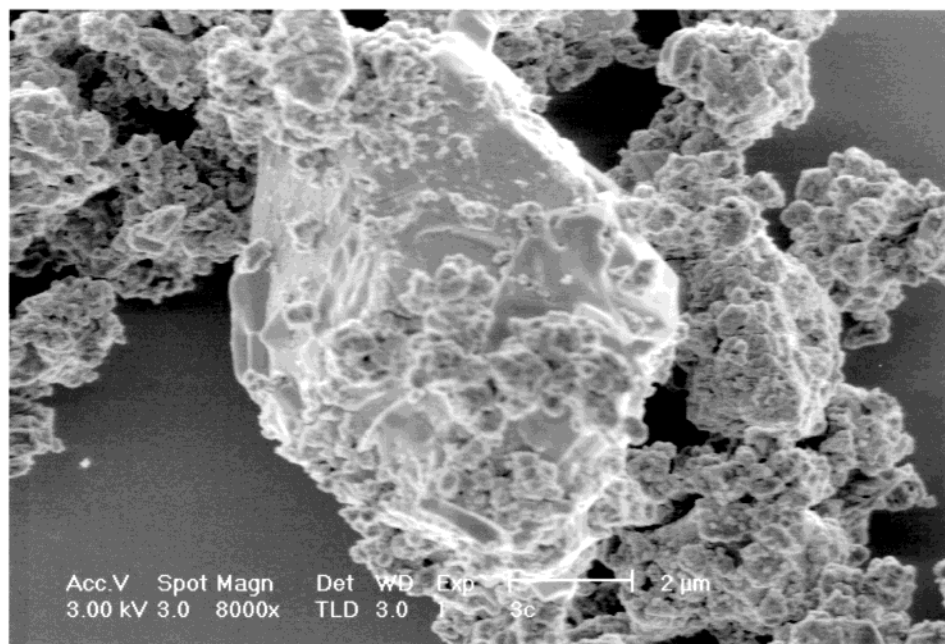
Figure 7. SEM image of a 3SrO/2TiO₂ mixture mechanoactivated for 11 days in the vibrating mill and then annealed at 800 °C for 24 h.

XRD data was approximately 12 nm, the same order of magnitude as obtained for $3SrO/2TiO_2$ mechanoactivation.

TG tracing of the powders milled for 14 days (Figure 2c) exhibited three important weight-loss steps: 14 wt % between room temperature and 100 °C, 2 wt % between 200 and 750 °C, and 4 wt % between 750 and 950 °C. The first loss of weight was well correlated with two endothermic peaks detected at 70 and 95 °C, also observed in the recording of the pure hydroxide. Furthermore, three other endothermic peaks were detected at 255, 470, and 884 °C, the two first being almost in the detection limit of the DTA technique.

XRD at increasing temperatures indicated the $SrTiO_3$ and $SrCO_3$ compounds, as in the as-milled powders, between room temperature and 700 °C. The intensities and peak widths of the $SrCO_3$ signals did not show any evident change even at the highest temperature. One can conclude that the weight loss and the DTA peaks observed between room temperature and 100 °C correspond to the thermal removal of water. However, the DTA maximum observed at 450 °C cannot be explained on the basis of the same phenomena. It is suggested that this peak corresponds to the removal of hydroxyl groups. Finally, the elimination of CO_2 at temperatures higher than 900 °C was accompanied by the partial crystallization of the Sr_2TiO_4 RP phase, which is in good agreement with the last endothermic peak (884 °C).

The products obtained after different furnace annealings are summarized in Table 1. Decomposition of $SrCO_3$ was achieved at temperatures higher than 900 °C, and prior to $Sr_3Ti_2O_7$ crystallization, the system passed through Sr_2TiO_4 phase formation. $Sr_3Ti_2O_7$ was obtained after an annealing treatment at 1250 °C for 120 h; however, a small peak at $2\theta \approx 40$ ° indicates that traces of $SrTiO_3$ were still present. Annealing treatments longer than 120 h only gave rise to $Sr_3Ti_2O_7$ degradation, going back to $SrTiO_3$.

When a $3Sr(OH)_2 \cdot 8H_2O/2TiO_2$ mixture was milled in the planetary mill the steel bowl and the balls were

eroded. We did no further work on this possibly contaminated sample.

Morphological Characterization. Only 2SrO/3TiO₂ mixtures were investigated by SEM, after both milling and annealing treatments. This approach was motivated by the fact that the optimized protocol for the $Sr_3Ti_2O_7$ RP synthesis was obtained from the strontium oxide precursor. Because of the high reactivity of SrO in air, it was not possible to investigate the initial mixture ($3SrO/2TiO_2$) previous to any mechanical milling.

Figure 6 shows the morphology of the powders obtained after different milling treatments. After 11 days of mechanoactivation in a vibrating mill (Figure 6a), one can observe conglomerates constituted by fine grains (∼100 nm in size) with irregular shapes; under these conditions, $SrTiO_3$ mechanosynthesis has been already observed by XRD. As the milling time increases to 14 days (Figure 6b), a large amount of the grains display a cubic symmetry, as expected for $SrTiO_3$. Their lateral sizes range approximately from 1 to 5 μm. These values are more than 2 orders of magnitude higher than the crystallite size measured by XRD (∼10 nm), corroborating the idea that, in most of these grains, the crystallographic structure is completely damaged. The presence of the conglomerates with irregular shapes indicates that a fraction of the powder has not yet reacted to form $SrTiO_3$, and more than one phase coexist. The occurrence of fine needles could indicate the presence of $SrCO_3$ or the fracture of $SrTiO_3$ grains.

In comparison to the vibrating mill, the planetary system has a greater effect on the morphology. After 7 days of mechanical treatment (Figure 6c), the powder is composed of agglomerates a few microns in size without any clear morphology. They have irregular shapes and are formed by the coalescence of grains that are hundreds of nanometers in size.

As expected, after different annealing times, there are important changes in the morphologies of the samples.

In fact, the precursors activated in the vibrating mill and heated at 800 °C for 24 h exhibit large grains with defined facets (Figure 7). The habit points to an orthorhombic symmetry and, therefore, might be related to the tetragonal $Sr_3Ti_2O_7$ RP phase detected by XRD. However, there remains a portion of material formed by small grains, similar to those observed in the untreated sample. These results suggest that the formation of the $Sr_3Ti_2O_7$ is not complete at this stage.

Conclusions

A comparative study concerning the synthesis of the $Sr_3Ti_2O_7$ RP phase was carried out using mechanoactivation routes.

Despite the use of different strontium reagents (oxide, carbonate, and hydroxide) and grinding techniques (vibrating and planetary mills), it was observed that there are common steps in the formation of the $Sr_3Ti_2O_7$ RP phase, during both mechanoactivation or calcination processes. They can be summarized as water adsorption/desorption, $SrCO_3$ formation/elimination, intermediate RP phase formation/mechanosynthesis ($n = 1$ and ∞), and finally crystallization of the $Sr_3Ti_2O_7$ compound. The optimum case is the synthesis protocol found by using SrO as the reagent. In fact, the mechanosynthesis of $SrTiO_3$ together with the formation of a small quantity of $SrCO_3$, makes this reagent much more attractive than $SrCO_3$ and $Sr(OH)_2 \cdot 8H_2O$.

It has been demonstrated that the synthesis protocol of the $Sr_3Ti_2O_7$ RP phase can be largely improved if the initial reagents are mechanoactivated. Mechanoactivation allows the temperature of formation to be lowered by approximately 450 °C when the SrO precursor is used. This can be attributed to the fracture of grains and defects generated during grinding, which leads to a higher internal energy, thus reducing the thermal budget required for any subsequent reaction. This strongly motivates an investigation of the production of new RP phases by means of the generalization of the synthesis protocol proposed in this paper. Furthermore, the homogenization of grain size would permit one to produce ceramics with more controllable compositions and microstructures as compared with the traditional ceramic routes.

CM0115012